Published by :
http://www.ijert.org

International Journal of Engineering Research & Technology (IJERT)
ISSN: 2278-0181
Vol. 14 Issue 09, September - 2025

Performance Analysis of PI and Sliding Mode Controllers with Hysteresis Current Control for Switched Reluctance Motor Drives : Simulation and Hardware Implementation

Abhijith S
M.Tech PE, Dept. of EEE
BMS College of Engineering,
Bull Temple Road,
Bengaluru-560019, KA, India

Dr. Padmavathi K
Professor Dept. of EEE
B.M.S College of Engineering,
Bull Temple Road,
Bengaluru-560019, KA, India

***Abstract*— Switched Reluctance Motors (SRMs) are emerging as promising candidate for electric vehicle (EV) propulsion systems because of their simple construction, fault-tolerant operation, and elimination of rare- earth permanent magnets. Despite these advantages, SRM drives inherently suffer from nonlinear dynamics and pronounced torque ripple, which limit their widespread adoption. This work presents a comparative evaluation of two control strategies – Proportional Integral (PI) control and Sliding Mode Control (SMC) -each integrated a hysteresis current controller for improved current regulation. Both controllers are designed, simulated and experimentally validated through hardware implementation. Experimental and simulation results show that PI + HCC ensures reliable steady-state operation, but SMC + HCC achieves superior dynamic response with reduced fluctuations. Such improvements make SMC-based control a strong candidate for EV-oriented SRM applications.**

***Keywords*— Switched Reluctance Motor (SRM), Electric Vehicle (EV), Proportional Integral (PI) control, Sliding Mode Control, Torque Ripple Reduction, Hardware Implementation**

I. INTRODUCTION

The demand for sustainable and efficient transportation has increased the adoption of electric vehicles (EVs). The performance of an EV largely depends on the choice and control of its propulsion motor. Among the available motor technologies, the switched reluctance motor (SRM) has received significant attention due to its simple construction, high fault tolerance, and independence from rare-earth permanent magnets [2], [7]. These features make SRMs a cost-effective option for reliable EV applications.

Despite these advantages, SRMs are limited by nonlinear magnetic characteristics and high torque ripple [4], [8]. These factors affect acoustic noise, driving comfort, and efficiency, and therefore restrict the widespread use of SRM drives. To address these issues, advanced control techniques are required to achieve smooth torque production and robust performance. Proportional–Integral (PI) controllers have been widely used in SRM drives because of their simplicity and ease of implementation [9], [10]. When combined with hysteresis current control (HCC), the PI scheme provides good steady-state accuracy and stable current regulation. However, PI controllers are sensitive to parameter variations and often show degraded performance under dynamic conditions [3], [10]. Sliding Mode Control (SMC) has been proposed as an alternative because of its robustness against uncertainties and nonlinearities [5], [11]. When integrated with HCC, SMC improves current regulation and dynamic response [6], [12], which is particularly beneficial for EV applications [13], [14]. This work presents a comparative study of PI + HCC and SMC + HCC controllers for SRM drives. The analysis is carried out through MATLAB/Simulink simulations and validated experimentally using a laboratory prototype. The results demonstrate that PI + HCC achieves satisfactory steady-state regulation, while SMC + HCC provides faster response and reduced current ripple, showing its potential as a more effective control strategy for SRM-based EV propulsion.

II. SYSTEM MODELLING AND CONTROL STRATEGY

A. Switched Reluctance Motor (SRM) Model

The Switched Reluctance Motor (SRM) is a doubly salient machine with independent stator phasor and no rotor windings or magnets. Its nonlinear electromagnetic nature makes control challenging [4], [8].

The voltage equation for a single phase is

$$v(t) = Ri(t) + \frac{d\varphi(i,\theta)}{dt}$$

Where:

v(t): phase voltage

R: phase resistance

i(t): phase current

$\varphi(i,\theta)$:flux linkage, dependent on current i and rotor position θ

The electromagnetic torque is given by:

International Journal of Engineering Research & Technology (IJERT)
ISSN: 2278-0181
Vol. 14 Issue 09, September - 2025

$$\mathrm{Te} = \frac{1}{2} i^2 \frac{\mathrm{dL}(\theta)}{\mathrm{d}\theta}$$

Where $L(\theta)$ is the position dependent inductance profile.

The mechanical dynamics are described as:

$$\mathrm{J}\frac{\mathrm{d}\omega}{\mathrm{dt}} + \mathrm{B}\omega = \mathrm{Te} - \mathrm{TL}$$

With J inertia, B damping , ω rotor speed and TL load torque.

B. PI + Hysteresis Current Control

In SRM Drives, PI controller is implemented in the speed control loop [9], [10]. The error is defined as:

$$e(t) = \omega^*(t) - \omega(t)$$

Where:

$\omega^*(t)$ is the reference speed.

$\omega(t)$ is the actual rotor speed.

The PI controller generates the current reference:

$$u(t) = K_p e(t) + K_i \int e(t)dt$$

Where K_p *and* K_i are the proportional and integral gains, respectively.

This output u(t) is treated as reference current $i^*(t)$. The hysteresis current controller(HCC) regulates the actual phase current i(t) such that it follows $i^*(t)$ within a predefined hysteresis band.

PI loop ensures accurate speed tracking and HCC loop provides fast current switching and torque generation [10].

C. SMC + Hysteresis Current Control

In the SMC strategy, the PI controller is replaced by an SMC [5], [11] speed controller, offering robustness against nonlinearities.

The sliding surface is defined as:

$$s(t) = \lambda e(t) + \frac{de(t)}{dt}$$

Where:

e(t) is the speed error.

λ is the design tunning parameter.

$\frac{de(t)}{dt}$ is the derivative of speed error.

The SMC control law is:

u(t) = *K*. sign(s(t))

where *K* is the control gain. This discontinuous law forces the trajectory onto the sliding surface (s(t) → 0).

The SMC output u(t) is used as the reference current $i^*(t)$, which is enforced by the hysteresis current controller [6], [12].in the inner loop.

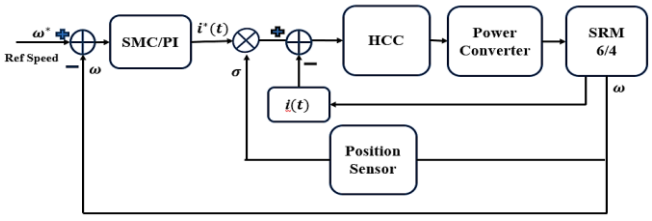

Fig. 1. Control architecture of the SRM drive with PI/SMC speed controller and hysteresis current control (HCC).

III. SIMULATION SETUP AND RESULTS

A. Simulation Setup

1) Motor parameters

The simulation of the 6/4 SRM drive was carried out in MATLAB/Simulink. The motor and controller parameters used are summarized in Table I.

Parameter	Value/Description
Motor type	6/4 Switched Reluctance Motor (SRM)
Converter DC link voltage	72 V
Maximum phase current	10 A (hardware rating; simulation limits were allowed to exceed this for analysis))
Load torque TL	2 Nm (constant)
Reference speed	1000 rpm (test case)
Unaligned inductance	0.297 mH
Aligned inductance	1.2 mH

TABLE I. MOTOR PARAMTERS IN SIMULINK MODEL

2) Controller Structures

Two control strategies were implemented for speed regulation of the SRM drive.

PI + Hysteresis Current Control (PI + HCC): The speed error, defined as the difference between the reference speed and the actual motor speed, is processed by the PI controller. The PI output generates the reference current, which is compared against the actual phase current in the hysteresis controller. The HCC ensures that the actual current follows the reference within a predefined hysteresis band, and generates the corresponding gate signals for the SRM converter [1], [5].

For PI control, the following parameters were used in simulation:

- Controller gains: *Kp* = 1, *Ki* = 0.62
- Commutation angles: Turn-on angle (α) = 44°, Turn-off angle (β) = 84°
- Modulation window: 90°

Sliding Mode Control + Hysteresis (SMC + HCC): In this approach, the PI speed regulator is replaced by a Sliding Mode Controller (SMC). The SMC constructs a sliding surface from the speed error and its derivative, and generates the control action accordingly. This control action is multiplied with the position sensor sigma signal, and the resulting reference current is enforced by the hysteresis controller [6], [7], [12].

International Journal of Engineering Research & Technology (IJERT)
ISSN: 2278-0181
Vol. 14 Issue 09, September - 2025

For SMC control, the setup parameters were:

- Commutation angles: Turn-on angle (α) = 35°, Turn-off angle (β) = 80°
- Modulation window: 90°

The PI and SMC yield different current build-up and demagnetization behavior; thus, their optimal commutation angles are not identical and were tuned separately to balance torque production and ripple [8], [10].

For both PI and SMC controllers, parameter tuning was carried out at 1000 rpm. This reference speed was used as the primary operating point to minimize steady-state error, while the same gains were tested at other speeds to assess general performance.

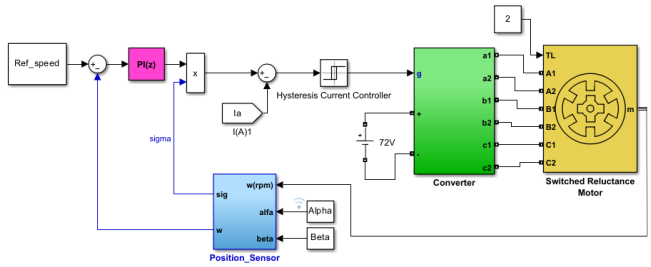

Fig. 2. Simulink model of SRM drive with PI + Hysteresis Current Control

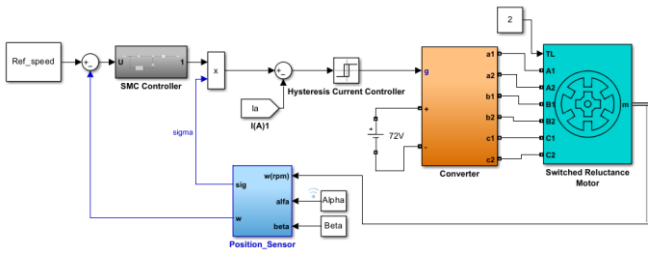

Fig. 3. Simulink model of SRM drive with SMC + Hysteresis Current Control

B. Simulation Results

The simulation studies were carried out for both PI + HCC and SMC + HCC controllers over reference speeds ranging from 200 rpm to 1000 rpm. The results were analysed in terms of speed regulation accuracy and phase current behaviour.

Fig. 4 and Fig. 5 show the comparison of reference and actual motor speeds under PI + HCC and SMC + HCC, respectively. In both cases, the actual speed followed the reference closely across the entire speed range, confirming effective regulation. The PI controller exhibited slightly slower dynamics, particularly at low speeds, while SMC provided smoother and faster convergence with negligible steady-state error.

The corresponding phase current responses are presented in Fig. 6 and Fig. 7. Under PI + HCC, phase currents remained within ~8 A at 1000 rpm, whereas SMC + HCC produced higher current magnitudes (~12–14 A) due to its stronger control action. This difference reflects the aggressive nature of SMC in minimizing error and enhancing robustness.

The numerical performance comparison at 1000 rpm is summarized in Table II. While both controllers maintained very low steady-state error (<0.2 rpm), PI + HCC showed higher current ripple, whereas SMC + HCC ensured smoother current tracking with stronger robustness to disturbances.

Controller	Steady-State Error (rpm)	Rise Time (s)	Overshoot (%)	Torque Ripple (%)
PI + HCC	0.10	0.0433	0.02	8.48
SMC+ HCC	0.15	0.0481	0.00	1.19

TABLE II. PERFORMANCE COMPARISON OF PI + HCC AND SMC + HCC AT 1000 RPM (SIMULATION)

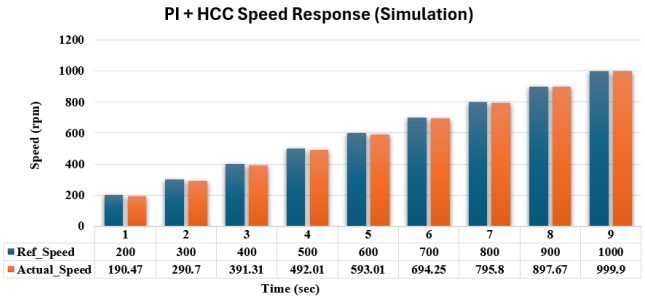

Fig. 4. Speed Response of SRM under PI + HCC

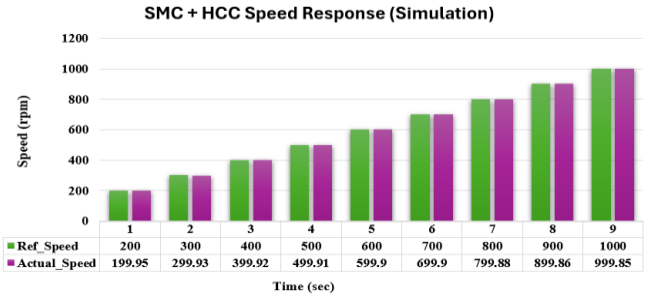

Fig. 5. Speed Response of SRM under SMC + HCC

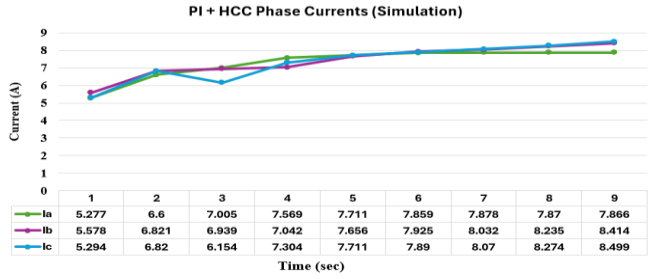

Fig. 6. Phase Currents of SRM under PI+ HCC

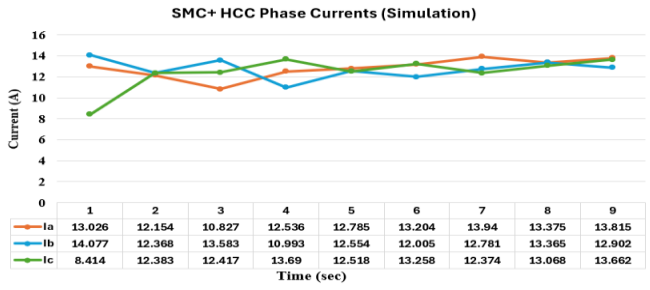

Fig. 7. Phase Currents of SRM under SMC + HCC

Published by :
http://www.ijert.org

International Journal of Engineering Research & Technology (IJERT)
ISSN: 2278-0181
Vol. 14 Issue 09, September - 2025

IV. HARDWARE SETUP AND EXPERIMENTAL RESULTS

A. Hardware Setup

The experimental system consists of a 6/4 SRM mechanically coupled to a DC machine. The input AC supply is first regulated using an autotransformer, which allows smooth variation of the supply voltage. This regulated AC is rectified by a diode rectifier to provide a stable DC link, which feeds a PWM inverter rated at 72 V, 10 A. The inverter excites the SRM phases with properly commutated currents.

The Wavect Tru-Control DSP platform (WCU300) generates the inverter switching signals. The DSP processes feedback from multiple ports, including rotor position from the encoder, phase currents, and voltages, and accordingly generates PWM gate pulses while ensuring protection features such as current and voltage limits. The controller includes built-in isolated PWM channels, high-resolution current and voltage measurement, and encoder interfaces, which simplify integration with the SRM drive. A PC interface (Wavect Suite) was used for parameter tuning, real-time signal monitoring, and experimental data acquisition [7]–[9].

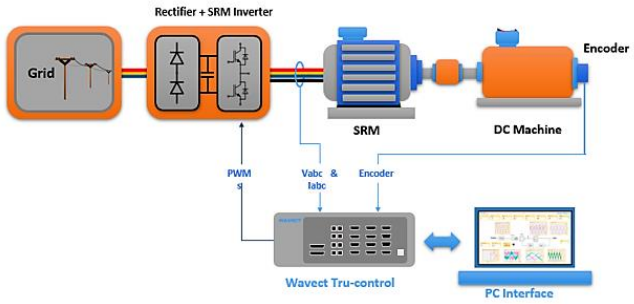

Fig. 8. Hardware Architecture of SRM drive system

The hardware architecture is shown in Fig. 8, while the physical laboratory setup is presented in Fig. 9. The overall system begins with the grid supply, regulated by the autotransformer, rectified by a diode bridge, and supplied to the SRM inverter. The SRM is mechanically coupled to a DC machine, while an encoder mounted on the shaft provides position feedback for commutation. The Wavect DSP interfaces with the inverter and measurement ports, handling PWM generation, data acquisition, and execution of the PI + HCC and SMC + HCC control strategies. This setup enabled direct validation of the control algorithms and comparison with simulation results.

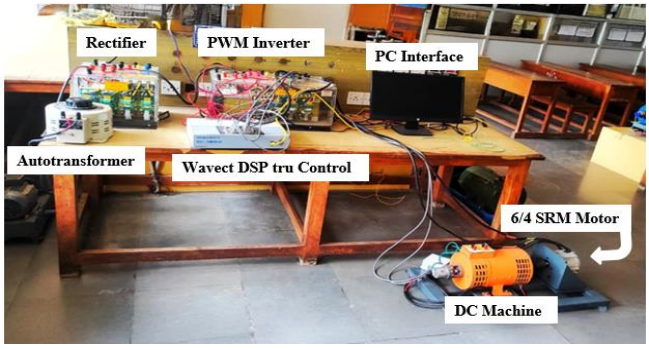

Fig. 9. Experimental Laboratory Setup.

B. Experimental Results

The experimental validation was carried out on the hardware setup described in Section IV-A. Both PI + HCC and SMC + HCC controllers were implemented on the 6/4 SRM, and the performance was evaluated under reference speeds ranging from 200 rpm to 1000 rpm.

Fig. 10 and Fig 11 show the comparison between reference speed and actual motor speed for PI + HCC and SMC + HCC controllers respectively [10], [11].

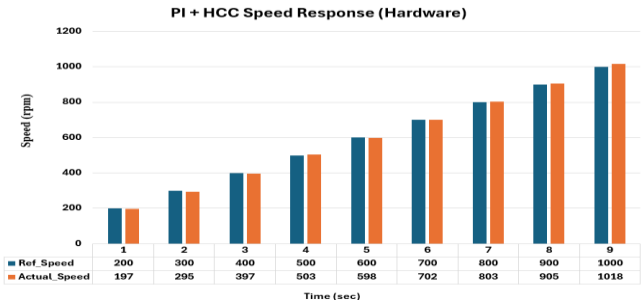

Fig. 10. Experimental speed response of SRM with PI + HCC controller

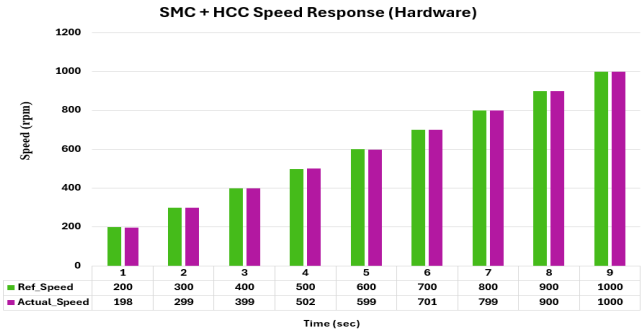

Fig. 11. Experimental speed response of SRM with SMC + HCC controller

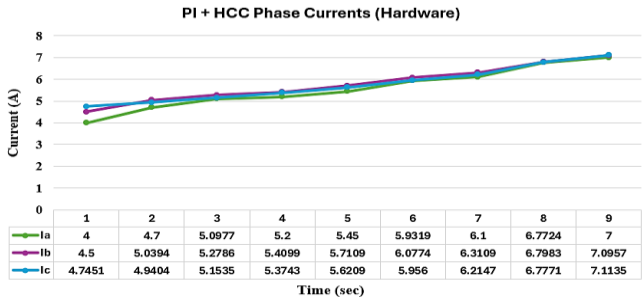

Fig. 12. Experimental Phase currents of SRM with PI + HCC controller

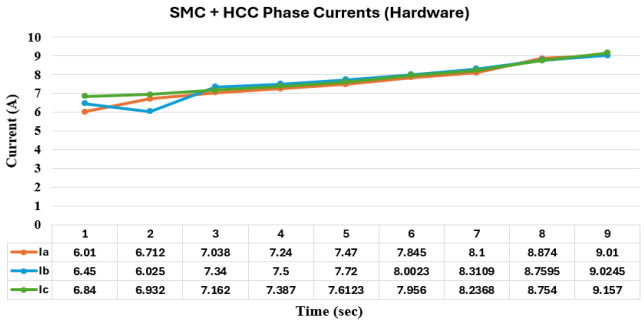

Fig. 13. Experimental Phase Currents of SRM with SMC + HCC controller

International Journal of Engineering Research & Technology (IJERT)
ISSN: 2278-0181
Vol. 14 Issue 09, September - 2025

In addition to speed tracking, the phase currents and voltages were also observed at different operating speeds. The measured current waveforms confirmed proper excitation of SRM phases, and the inverter switching was verified from the voltage signals. Representative current responses are shown in Fig. 12 and Fig. 13, respectively.

The measured phase currents increased with speed, reaching ~ 7 A for PI and ~9 A for SMC at 1000 rpm. Converter voltages were also recorded (ranging from ~9 V at 200 rpm to ~17 V at 1000 rpm) and confirmed to be within the 72 V, 10 A converter rating. However, only current waveforms are presented here for brevity [12].

Controller	Final Speed (rpm)	Deviation from Ref (rpm)	Phase Current (RMS)
PI + HCC	~1018	+18	~7A
SMC+ HCC	~1000	+0	~9A

TABLE III. PERFORMANCE COMPARISON OF PI + HCC AND SMC + HCC AT 1000 RPM (HARDWARE)

In hardware experiments at 1000 rpm reference, the PI + HCC controller showed a final speed reaching ~1018 rpm, indicating a positive deviation of about +18 rpm. The PI speed response also exhibited small fluctuations around the steady state. In contrast, the SMC + HCC controller consistently maintained the actual speed close to the reference (~1000 rpm) with significantly smaller deviations. The phase current levels were higher under SMC (~9–10 A) compared to PI (~7–8 A), reflecting stronger control action and faster dynamic response.

- PI + HCC: Achieved good steady-state accuracy but exhibited slightly slower dynamic response compared to simulation.
- SMC + HCC: Demonstrated faster convergence and smoother tracking, consistent with the simulation results.

It is important to note that torque measurements were not recorded in the hardware experiments due to the absence of a torque sensor. Nevertheless, current and voltage waveforms were monitored at different speeds to confirm proper converter switching and phase commutation.

Overall, the hardware results validate the simulation outcomes, with SMC + HCC providing superior performance in terms of dynamic response and robustness, while PI + HCC ensured reliable steady-state speed regulation [10]– [14].

V. CONCLUSION

This paper has presented a comparative study of PI + HCC and SMC + HCC controllers applied to a 6/4 SRM drive. Both control strategies were implemented in MATLAB/Simulink and tested on a 72 V, 10 A laboratory prototype for validation [3], [7]. The results confirmed that both controllers are capable of maintaining accurate speed regulation under different operating conditions.

From simulation, the PI + HCC controller showed higher torque ripple (≈8–10%) and larger transient overshoot, whereas SMC + HCC maintained ripple below 2% and achieved faster convergence with no overshoot [5], [6], [12].

In hardware, torque was not directly measured, but speed and current responses supported the same trends. PI + HCC provided stable steady-state operation but with minor fluctuations, while SMC + HCC delivered smoother tracking and closer speed regulation [4], [9].

In summary, PI controllers remain attractive for their simplicity and straightforward tuning [1], [2], but the improved robustness and dynamic performance of SMC make it a stronger option for EV drive applications, where torque smoothness and speed accuracy are critical [5], [11]. Future work will explore advanced techniques such as Model Predictive Control (MPC) and optimization-based methods including GA, PSO, DE, and AIS for further reduction of ripple and improved system efficiency [13]–[15].

REFERENCES

[1] H. A. Toliyat, M. Rahman, and R. Krishnan, Advances in Switched Reluctance Motor Drives and Applications. Springer, 2021.
[2] C. Gan, J. Hu, W. Cao, Y. Hu, and J. Wu, “Advances in control of switched reluctance machines for electric vehicle applications: State of the art and future trends,” IEEE Trans. Ind. Electron., vol. 68, no. 6, pp. 5026–5039, Jun. 2021.
[3] R. Krishnan, Switched Reluctance Motor Drives: Modeling, Simulation, Analysis, Design, and Applications. CRC Press, 2017.
[4] A. Radun, “Analytical calculation of the torque ripple in switched reluctance motors,” IEEE Trans. Energy Convers., vol. 16, no. 1, pp. 24–30, Mar. 2001.
[5] B. K. Bose, “Sliding mode control in electric drives,” Proc. IEEE, vol. 82, no. 8, pp. 1205–1219, Aug. 1994.
[6] Z. Chen, Y. Zhang, and C. Gan, “Sliding mode and predictive torque control of switched reluctance motor drives for electric vehicles,” IEEE Trans. Power Electron., vol. 36, no. 9, pp. 10645–10658, Sep. 2021.
[7] M. Ehsani, Y. Gao, and S. Gay, Modern Electric, Hybrid Electric, and Fuel Cell Vehicles. CRC Press, 2018.
[8] S. R. MacMinn and T. M. Jahns, “Control techniques for improved performance of switched reluctance motors,” IEEE Trans. Ind. Appl., vol. IA-22, no. 5, pp. 837–843, Sep. 1986.
[9] K. R. Rajagopal and B. Fahimi, “Application of PI controllers for switched reluctance motor drives,” IEEE Trans. Ind. Electron., vol. 49, no. 1, pp. 165–171, Feb. 2002.
[10] G. K. Singh, “Comparison of PI and hysteresis current controllers for SRM drives,” IET Electr. Power Appl., vol. 4, no. 3, pp. 174–184, Mar. 2010.
[11] V. Utkin, “Variable structure systems with sliding modes,” IEEE Trans. Autom. Control, vol. 22, no. 2, pp. 212–222, Apr. 1977.
[12] S. Sun, C. Gan, and Y. Hu, “Improved sliding mode control for torque ripple reduction in switched reluctance machines,” IEEE Access, vol. 8, pp. 125870–125882, 2020.
[13] P. Li, L. Xu, and J. Wu, “Experimental validation of torque ripple reduction in SRM drives using advanced controllers,” IEEE Trans. Energy Convers., vol. 35, no. 4, pp. 2074–2084, Dec. 2020.
[14] M. Hannan, J. Lipu, A. Hussain, and A. Mohamed, “Comparative performance analysis of PI, SMC, and predictive controllers for switched reluctance motors in EVs,” IEEE Trans. Veh. Technol., vol. 69, no. 11, pp. 12645–12656, Nov. 2020.
[15] A. Manjula, L. Kalaivani, and M. Gengaraj, “PSO Based Torque Ripple Minimization Of Switched Reluctance Motor Using FPGA Controller,” Intelligent Automation & Soft Computing, vol. 29, no. 2, pp. 42935–42958, 2021.